23 Accelerator Mass Spectrometry

L.K. Fifield

Department of Nuclear Physics, Research School of Physical Sciences and
Engineering, Australian National University, ACT 0200, Australia
`keith.fifield@anu.edu.au`

23.1 Introduction

Accelerator mass spectrometry (AMS) is a mass-spectrometric technique
which incorporates an accelerator to achieve much higher sensitivities than
are attainable with conventional mass spectrometers.

Usually, the atoms to be counted are radioactive with a long half-life,
and are rare. The archetypal example is ^{14}C, which has a half-life of 5730
years and an abundance in living organisms of 10^{-12} relative to stable ^{12}C.
Using AMS, the radiocarbon age of a sample less than $10\,000$ years old can
be determined to a precision of 0.5% in a few minutes using a milligram or
less of carbon. The sensitivity, which is more relevant than precision for very
old or very small samples, is $\sim 10^4$ atoms of ^{14}C.

The utility of AMS is not limited to ^{14}C alone, however, and many other
isotopes are amenable to the technique, the most important of which are ^{10}Be
($T_{\frac{1}{2}} = 1.5\,Ma$), ^{26}Al (720 ka), ^{36}Cl (301 ka) and ^{129}I (15 Ma).

AMS emerged from nuclear-physics laboratories with electrostatic tan-
dem accelerators in the late 1970s. The first AMS observations of ^{14}C from
natural materials were reported simultaneously by two groups, one working
at McMaster and the other at Rochester [1,2].

Following these first successful demonstrations, dedicated AMS systems
based on the Mark I Tandetron [3] were soon developed, and the first three
were installed at Arizona, Oxford and Toronto in 1981–82. At the same time,
several nuclear-physics laboratories added an AMS component to their re-
search programs, and a number of these have evolved into dedicated AMS
facilities. Techniques for other isotopes, in particular ^{36}Cl [4], ^{129}I [5], ^{10}Be [6]
and ^{26}Al [7], were soon developed.

Beginning in about 1990, a series of second-generation purpose-built sys-
tems operating at $3\,MV$ have had a major impact on the field. Subsequently,
the development of systems based on small accelerators operating at $0.5\,MV$
or less is bringing high-precision, high-throughput AMS for radiocarbon
within reach of more laboratories. There are presently (2003) about 50 lab-
oratories worldwide which are actively involved in AMS.

In parallel with the growth in the number of facilities, applications of the
technique have burgeoned. Traditional ^{14}C dating is no longer the dominant
application. Carbon-14 remains the most important isotope, but much of the

research is now directed towards an understanding of global climate change via studies of oceanic circulation, atmospheric processes and past climates. Biomedical applications of ^{14}C are also becoming increasingly important. Cosmic-ray exposure dating, which exploits the buildup of ^{10}Be, ^{26}Al or ^{36}Cl in surface rocks, is making an increasingly significant contribution to studies of landscape evolution and paleoclimates. Beryllium-10 has also been used in studies of soil processes, the deposition of ocean sediments, and the sources of volcanic rocks. Both ^{36}Cl and ^{129}I have been used in hydrology and in tracing the migration of nuclear waste, while ^{26}Al and ^{41}Ca have found application in biomedicine. New applications continue to surface, often spawning new developments in technique.

In this review, I shall concentrate on the current state of the art in AMS technique, and on recent innovations. The principal areas of application of AMS will be briefly surveyed to give a flavor of the science. More detail can be found in earlier reviews [8–11].

23.2 Principles of Accelerator Mass Spectrometry

23.2.1 The Need for AMS

For rare, long-lived radioisotopes, AMS overcomes certain fundamental limitations of both decay-counting and conventional mass spectrometry. These limitations are best illustrated using the familiar example of ^{14}C.

There are 6×10^{10} atoms of ^{14}C in 1 g of modern carbon, but only 14 decay per minute. In order to achieve 0.5% statistical precision with decay counting, it would be necessary to count for at least 48 hours.

A mass-spectrometric method could in principle count a much higher fraction of the ^{14}C atoms in a sample than decay-counting. Conventional mass spectrometers are not practicable, however, because the ^{14}C ions are masked by relatively intense fluxes of ions of the ^{14}N isobar, by background from tails of the stable isotopes ^{12}C and ^{13}C, and also by molecular ions such as ^{13}CH, ^{12}CH$_2$, ^{12}CD and ^{7}Li$_2$. As outlined below, all of these limitations are overcome in an accelerator mass spectrometer.

In marked contrast to decay-counting, typical ^{14}C counting rates in an AMS system are $\sim$100 s^{-1}, and only 1 mg of carbon is sufficient for a measurement.

23.2.2 Principles of AMS

Accelerator mass spectrometry combines the high efficiency of mass spectrometry with excellent discrimination against isobaric, isotopic and molecular interferences. It achieves this by:

– using negative ions
– dissociating molecular ions after a first stage of acceleration
– identifying individual ions after a second stage of acceleration and analysis.

Figure 23.1 shows a schematic representation of an accelerator mass spectrometer. Each of its essential features is described in sequence below. Details specific to individual isotopes will be taken up later.
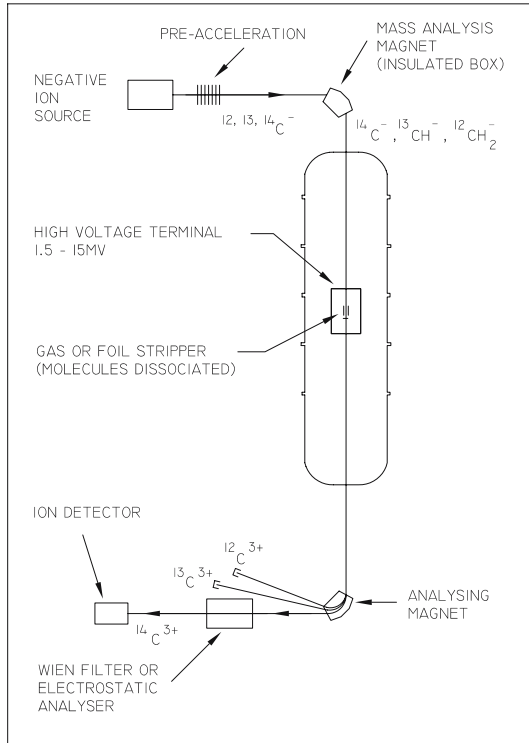

Fig. 23.1. The essential features of an AMS system. Mass-14 ions are shown being transmitted around the mass-analysis magnet. Periodically or simultaneously, mass-12 and mass-13 ions are transmitted, and measured in the off-axis cups after the analyzing magnet

– Negative ions are generated from the sample in a cesium sputter source, preaccelerated to 30–200 keV and mass-analyzed by a magnet. In the cases of ^{14}C, ^{26}Al and ^{129}I, the choice of negative ions eliminates the isobaric interferences because ^{14}N, ^{26}Mg and ^{129}Xe do not form stable negative ions.
– The mass-analyzed negative ions are accelerated to the positive high-voltage terminal of the tandem accelerator, where they pass through a gas

or foil stripper. A crucial role of the stripper is to dissociate any interfering
molecular ions.

– The now positively charged ions are further accelerated back to ground
potential in the second stage of the tandem accelerator. Subsequent mag-
netic and electric analyzers select the ions of interest with a well-defined
combination of charge state and energy.
– Individual ions are identified and counted by a detector. Identification is
necessary because ions other than those of the AMS isotope may also reach
the detector.
– Generally, AMS determines the abundance ratio of the rare isotope to a
stable abundant isotope of the same element, $^{14}C/^{12}C$ for example, by also
measuring the flux of the abundant species as an electrical current in a
Faraday cup after acceleration.

The above gives the bare essentials of an AMS system. In the following,
the various components are considered in somewhat more detail.

The Ion Source

AMS ion sources are almost exclusively cesium sputter sources (see Chap.
12). Most are "high-intensity" sources, in which the hot tantalum ionizer
and the sample are within the same volume containing Cs vapor, although
some Cs-gun-type sources are still employed. The majority are either the 846
model source from HVEE, which has a 60-sample carousel, or the MC-SNICS
manufactured by NEC, which is available with either a 40- or a 134-sample
wheel. In both sources, the carousel or wheel can be replaced through a vac-
uum lock in order to minimize downtime. In the HVEE source, it is possible
to move the sample relative to the Cs beam to avoid cratering and to utilize
the sample material efficiently. Driven by the need for both higher through-
put and higher precision, significant progress has been made in understanding
and improving these sources, and $^{12}C^-$ currents as high as $200\,\mu A$ have been
achieved from graphite samples. Typical negative-ion beam currents for the
species commonly used in AMS are given in Table 23.1.

Table 23.1. Typical beam currents from high-intensity cesium sputter sources used
for AMS

AMS Isotope	Material	Selected Ion of Stable Isotope	Negative-ion Current (μA)
^{10}Be	BeO	$^{9}Be^{16}O^-$	1–20
^{14}C	Graphite	$^{12}C^-$	20–100
^{26}Al	Al_2O_3	$^{27}Al^-$	0.1–1
^{36}Cl	AgCl	$^{35}Cl^-$	5–25
^{129}I	AgI	$^{127}I^-$	2–10

At Oxford, a source which uses CO_2 as well as graphite has been in operation for several years [12], and similar sources are beginning to appear in other laboratories. In this case, the disadvantage of lower beam currents ($\sim 10\,\mu A$) is compensated by the substantial simplification in sample preparation and the capability to run samples as small as a few μg.

The Injection System

Specialized injection systems have been developed in order to inject both the rare and the abundant isotopes into the accelerator.

In a sequential system, switching between isotopes is accomplished by changing the energies of the negative ions in the mass-analysis magnet after the ion source. This is achieved by applying different voltages to the electrically isolated vacuum box of the magnet. In order to minimize the effect of fluctuations in the ion source output, switching times should be short and repetition rates high. Switching times down to μs are employed, and typical repetition rates are $10\,s^{-1}$, with >90% of the time spent on the rare isotope. Typically, the very intense stable beams are pulsed into the accelerator for $100\,\mu s$ or less in order to avoid beam-loading effects. Electrostatic lenses at the beginning and end of the insulated section are required to ensure identical trajectories of the different isotopes.

Alternatively, the stable and radioactive isotopes can be injected simultaneously. Simultaneous-injection systems employ a sequence of dipole magnets and lenses which allow the different isotopes to follow different trajectories after leaving the ion source before being recombined at the entrance to the accelerator. This approach was pioneered at McMaster [13] and has been adopted for the Mark II Tandetron systems [14]. The recombinator for the latter machines, which are used almost exclusively for ^{14}C, is depicted in Fig. 23.2. Attenuation of the intense ^{12}C beam is accomplished by interposing a rotating slotted wheel in its path where the separation of the isotopes is a maximum.

In either case, the beam currents of the stable beams are measured in off-axis Faraday cups after the postacceleration analyzing magnet (Fig. 23.1).

The Accelerator

The appropriate size of accelerator is determined by the following two factors.

– *The charge state of the positive ions.* Until recently, it was widely accepted that the minimum charge state for AMS was 3^+. This was based upon the fact that some singly or doubly charged molecular ions are stable, $^{13}CH^+$ and $^{12}CH_2{}^{2+}$ for example. If these were to survive the stripping process, and at the gas stripper pressures typically employed, some certainly do, they would be essentially indistinguishable from ^{14}C with the same charge
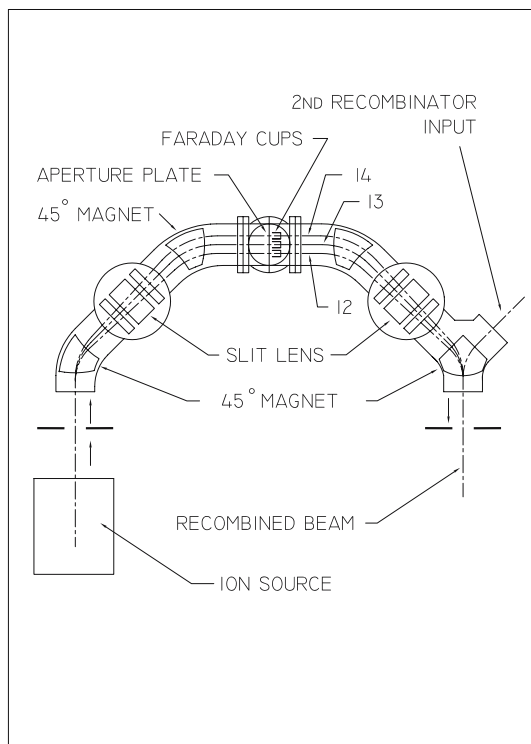
Fig. 23.2. The recombinator injection system used by AMS systems based on Mk II Tandetrons

state. Hence, they were thought to preclude the use of 1^+ or 2^+ ions, not only for ^{14}C, but for all AMS isotopes. Since the 3^+ stripping yield for carbon is appreciable only above 2 MeV, the requirement was for accelerators operating at 2 MV or more.

In one of the major advances in AMS of the past few years, the Zürich group has demonstrated [15] that it is possible to dissociate essentially all of the ^{13}CH and ^{12}CH$_2$ molecules at gas stripper thicknesses of $\sim$2 μg/cm^2. The original demonstration employed a 500 kV accelerator and the 1^+ charge state, but subsequently the Zürich group has taken miniaturization a step further by showing the feasibility of a system with a footprint of only 3×2.3 m^2 based on a 200 kV vacuum-insulated accelerator. In parallel, NEC have developed a system employing only a single stage of acceleration to 300 kV across a standard air-insulated acceleration tube. The gas stripper, final analysis stages and detector are all at high voltage. Both systems utilize commercial high-voltage power supplies.

– *Ion identification.* For some AMS isotopes, the choice of negative ions does not exclude the isobar. The best-known example is ^{36}Cl, where negative

ions of the ^{36}S isobar are produced equally readily in the ion source, and inevitably accompany the ^{36}Cl all the way to the final detector. Discrimination of a few ^{36}Cl ions in the presence of a much greater flux of ^{36}S ions is only possible at energies above ∼50 MeV, and hence AMS of ^{36}Cl requires larger accelerators.

The tandem electrostatic accelerators employed in AMS may therefore be conveniently grouped into four categories on the basis of their maximum terminal voltage V_T.

1. $V_T < 1$ MV. Following the successful demonstration that radiocarbon AMS was possible using 1^+ ions, several systems based on a 500 kV accelerator have now been delivered by NEC or are on order. Although they are presently being used almost exclusively for high-precision radiocarbon measurement, their potential for other isotopes is being actively explored by the Zürich group, and promising results for ^{10}Be, ^{26}Al, ^{41}Ca, ^{129}I and plutonium have been reported [16, 17].

2. $1 < V_T < 3$ MV. This category includes the Tandetrons, now manufactured by HVEE, and 3 MV accelerators from NEC, and presently constitutes the majority of dedicated AMS systems. They are predominantly used for high-precision ^{14}C measurements, but also for ^{10}Be, ^{26}Al and ^{129}I. The Tandetrons are charged by a radio-frequency voltage-doubling power supply.

3. $4.5 < V_T < 9$ MV. Machines in this category are principally extensively modified ex-nuclear-physics accelerators, predominantly EN and FN accelerators manufactured by HVEC in the 1960s and 70s. More recently, NEC have entered this category with a purpose-built 5 MV system, of which four have been delivered. HVEE also now offer a 5 MV Tandetron system. Essentially the full range of AMS isotopes can be covered by accelerators of this size, although the separation of ^{36}Cl from ^{36}S is challenging at less than 6 MV.

4. $V_T > 10$ MV. These are operational nuclear-physics accelerators on which AMS typically takes 20% of the beam time. Modifications to the injection system or accelerator specifically for AMS are usually minimal. The higher energies available from these larger machines are particularly advantageous for ^{36}Cl and for isotopes requiring a gas-filled magnet. In addition, much of the development of new isotopes has been carried out on them. They include the NEC 14UD Pelletron and the HVEC MP and XTU accelerators.

The desirable criteria for an AMS accelerator are that transmission of ions through the accelerator should be high and reproducible, that this transmission should be insensitive to small changes in the injection or accelerator parameters, and that the terminal voltage should be very stable. High and flat-topped transmission is achieved by using large-diameter acceleration tubes, spacious vacuum chambers within magnets, and apertures which are

as large as possible. Ion-optical transmission is typically >80% in dedicated AMS systems. Consistency of transmission is best achieved using gas stripping in the high-voltage terminal, and most of the facilities which aim at high-precision ^{14}C use an argon gas stripper. Gas stripper canals are typically 8 mm in diameter and may constitute the smallest restriction in the system. Careful attention to ion optics is therefore required to ensure that transmission losses are minimal.

Stabilization of the accelerator's terminal voltage presents a particular challenge. The usual slit-stabilization method, which depends on nA currents striking slits after the final analyzing magnet, is not applicable, since there are typically only a few ions per second of the AMS isotope. Two solutions have been adopted. Either the signal from a generating voltmeter (GVM) is used, or the off-axis position of one of the stable beams is monitored by a Faraday cup which is split in two to give separate left and right signals [18]. The former is the more widely used and is capable of excellent stability. For example, the fluctuations in the terminal voltage of the 14UD accelerator at the Australian National University are ∼1 kV in 14 MV under GVM stabilization. Of course, it helps if the accelerator is intrinsically very stable, and Pelletron charging systems and the solid-state power supplies of the Tandetrons have distinct advantages over the older rubberized belts in this regard.

Postacceleration Analysis

Following acceleration, the charge state and energy of interest are selected by magnetic analysis. The stable isotopes have different radii of curvature and are collected in off-axis Faraday cups at the focal plane of the magnet. At the exit from a typical 1 m radius analyzing magnet, the separation between ^{12}C and ^{14}C is 8 cm, and hence purpose-built magnets with wide pole pieces at the exit are required to accommodate the different ion species.

An additional analysis stage, either an electrostatic analyzer or a velocity filter, follows the analyzing magnet to remove that small fraction of molecular fragments which has acquired the correct energy to follow the same trajectory as the AMS isotope through the magnet. These can otherwise cause unacceptably high counting rates in the ion detector. Rates depend on the vacuum in the high-energy acceleration tube, and because some unwanted ions inevitably leak through even the additional analysis stage, the higher the vacuum the better. To this end, gas strippers which employ turbomolecular pumps in the high-voltage terminal to recirculate the gas [19] are now widely employed, and high-pumping-speed cryopumps or turbomolecular pumps are installed as close as possible to the end of the high-energy tube. Acceleration tubes of the NEC design, in which ceramic insulators are bonded without adhesives to titanium electrodes, offer advantages in terms of higher vacuum over the more widely used tubes in which glass insulators are bonded to metal electrodes with organic adhesives.

Detectors

A range of ion detectors have been variously employed to count the AMS isotope.

– *Silicon detectors.* These measure only the energy of the ion. In some cases, this is sufficient for unique identification of the AMS isotope, since any background ions have a different mass and therefore energy. A drawback of silicon detectors is that they are susceptible to radiation damage.
– *Ionization chambers.* Ionization chambers are more robust, and can measure not only the total energy of an ion but also its rate of energy loss as it slows down in the detector gas. A typical multielement ionization chamber is depicted in Fig. 23.3. Until recently, gas-confining windows were almost exclusively Mylar, typically $1.5\,\mu\mathrm{m}$ thick, but the advent of silicon nitride windows with thicknesses as low as $0.03\,\mu\mathrm{m}$ seems set to confer substantial gains in energy resolution, especially for low-energy heavy ions. Propane, isobutane and P-10 (90% argon, 10% methane) are the usual counter gases employed. Isobutane has the advantage in some applications of a higher stopping power but is comparatively expensive, while propane is cheap and readily available. Electrons produced by the passage of the energetic ion drift towards the anode in the transverse electric field. The anode is subdivided into sections, each of which collects those electrons produced beneath it, thereby measuring the energy lost by the ion along that portion of its track. Since ions of different Z lose energy at different rates, this
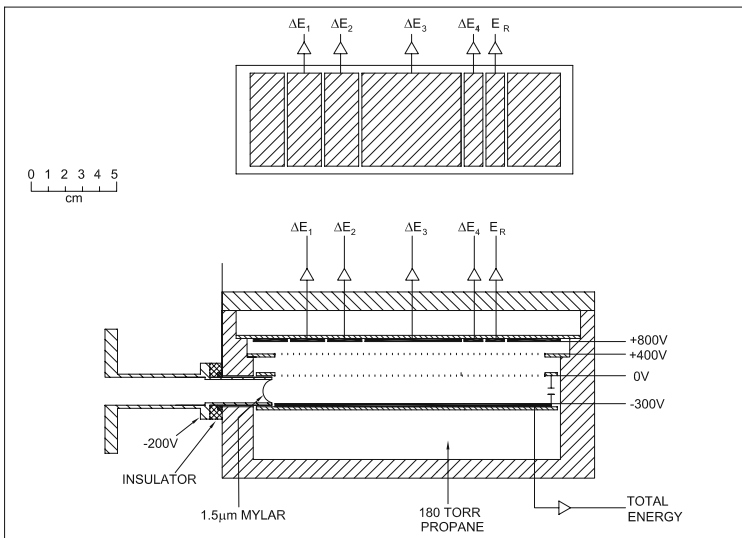

Fig. 23.3. A cross section through the multielement ionization chamber used at the Australian National University. The *upper* panel shows a plan view of the anode electrode

energy-loss information permits the separation of isobars, ^{36}Cl and ^{36}S for example, which have identical energies when they arrive at the detector. Issues specific to certain isotopes will be taken up in Sect. 23.3.

Hybrid detectors, which employ a gas ionization chamber for energy-loss measurement and a silicon detector to measure the residual energy, have also been used [20].

– *Time-of-flight systems.* For heavier ions, the energy resolution of an ionization chamber or silicon detector is insufficient to resolve neighboring masses. Better separation is possible by combining the energy measurement with a determination of the ion's velocity via a time-of-flight measurement. Such systems have been used for ^{129}I, and for very heavy isotopes such as ^{236}U.

A time-of-flight system consists of "start" and "stop" detectors separated typically by 2 m. Start detectors invariably consist of a thin carbon foil and a microchannel plate, which multiplies the electrons liberated from the foil by the passage of the ion. The stop detector may be similar to the start detector, in which case it is backed by a silicon detector or ionization chamber for energy measurements. Alternatively, a silicon detector (which may be part of a hybrid system) is often used to provide both timing and energy signals. Typical time resolutions achieved with such devices are 300–500 ps, which is more than adequate to separate ^{129}I from ^{128}Te and ^{127}I.

A drawback of time-of-flight systems is the loss of efficiency associated with scattering from grids and from the start foil, and efficiencies typically range between 50 and 80%. Scattering from the foil is crucially dependent on the foil thickness, and diamond-like carbon foils as thin as $0.5\,\mu\text{g/cm}^2$ are now available.

– *Gas-filled magnets.* Isobars, which have the same mass and energy after acceleration, may be separated by passage through a gas-filled region within a magnetic field. Owing to the difference in Z, their average charge states are different in the gas-filled region, and hence they follow different trajectories in the magnetic field. The unwanted, high-counting-rate isobar can then be intercepted by an appropriately positioned baffle. The AMS isotope continues to an ionization chamber which distinguishes between the AMS isotope and events due to tails of the isobar distribution. An excellent review of gas-filled magnets as applied to AMS has been given by Paul [21]. Purpose-built systems have been installed at Zürich [22] and Munich [23]. Existing magnetic spectrometers have also been pressed into service [24].

– *X-ray detectors.* Fast ions may be identified by the characteristic X-rays they emit following excitation in a foil, thereby allowing isobar separation at energies where ionization chambers give rather poor discrimination. This technique has been applied to the detection of several isotopes, including ^{36}Cl, ^{59,63}Ni, ^{60}Fe, ^{79}Se and ^{126}Sn [25–27]. The optimal foil material has $Z_{\text{foil}} \approx Z_{\text{ion}} + 2$, and X-ray yields are strongly dependent on energy. At the

energies obtainable from a 9 MV accelerator, yields vary from one X-ray per incident ion for light ions such as Si to one X-ray per 300 incident ions for ^{106}Pd [27]. Only a fraction of these X-rays are actually detected, however, owing to the limited solid angle subtended by the detector and an intrinsic detector efficiency of less than unity.

23.3 Techniques for Individual Isotopes

Each AMS isotope is a little different, and has its own special considerations and refinements of technique. These are discussed below.

23.3.1 Carbon-14 ($T_{\frac{1}{2}} = 5730$ a)

Applications of ^{14}C place more stringent demands on precision than any other isotope, and a precision of 0.3%, corresponding to 25 years in radiocarbon age, is presently the benchmark for dedicated AMS laboratories. In order to attain this level of precision it is necessary, first, to obtain sufficient ^{14}C counts that the statistical uncertainty is at the desired level, and, second, to achieve a high degree of reproducibility.

In order to achieve a statistical uncertainty of 0.3%, 150 000 counts are required, both for the sample of unknown age and for the standard relative to which it is measured. Since the ^{14}C counting rate from a 5000-year-old sample is typically 70 s^{-1}, a sample of this age must be run for at least 30 minutes to obtain the requisite number of counts. This count rate assumes a source output of 50 μA of ^{12}C^{-}, a charge state fraction of 50% and ion-optical transmission of 80%. Generally, the requisite number of counts will be accumulated over a number of runs interleaved with standards and other samples, allowing an estimate of the external error and hence a check on the reproducibility of the system.

Good reproducibility requires that transmission be insensitive to small changes in any of the system parameters. Considerable care is therefore taken during setting up to ensure flat-topped transmission in all parameters.

Modern systems incorporate a high level of automation to control not only the fast-cycling sequence, but also the sequencing of samples and, increasingly, automated tuning. Unattended operation for the duration of a complete wheel or carousel of samples is becoming commonplace. In addition, the computer control program maintains a watch on the integrity of the data by continuously monitoring the ratios of the different isotopes as a measurement proceeds. Possible problems can then be identified and flagged for later consideration, or an operator alerted.

For high-precision dating, it is necessary to correct for the natural fractionation inherent in biological processes. Carbon from C3 plants (e.g. forest trees) is depleted by 1.5% in ^{13}C relative to C4 plants (most grasses), which

are in turn depleted by 1% relative to marine organisms. Hence, in addition to the AMS measurement of the $^{14}C/^{12}C$ ratio, a measurement of the $^{13}C/^{12}C$ ratio is also required. In the past, the $^{13}C/^{12}C$ ratio was usually measured off-line on a subsample of CO_2 with a conventional mass spectrometer because the measurement of this ratio by the AMS system was insufficiently precise. Modern systems, however, now achieve precisions of 2 per mil or better in the AMS measurement of the $^{13}C/^{12}C$ ratio, thereby avoiding the extra step. An additional benefit is that any fractionation introduced during conversion of the sample to graphite or in the ion source is automatically accounted for.

23.3.2 Beryllium-10 ($T_{\frac{1}{2}} = 1.50\,\text{Ma}$)

Beryllium does not form a stable atomic negative ion. Samples are therefore prepared as beryllium oxide and the BeO^- molecular ion is selected for analysis. Currents of several μA are obtained, and can be enhanced by mixing the BeO with niobium metal powder [28].

At the stripper, the ^{10}Be atom carries only 10/26 of the energy of the molecular ion and thus strips to a lower average charge state than if it had the full energy. Hence, the 2^+ charge state is employed on the smaller machines operating at 2–3 MV, and the 3^+ charge state on larger accelerators operating at >5 MV. In the latter case, a foil stripper following the gas stripper leads to a higher yield of the 3^+ charge state. A foil stripper alone is not suitable, because "Coulomb explosion" of the molecule as it breaks up in the foil results in substantial losses due to increased divergence and energy spread.

Boron-10 is the stable isobar of ^{10}Be. It readily forms BO^- ions, and hence ^{10}B ions inevitably accompany the ^{10}Be ions after acceleration. Despite the best efforts of the chemist, typical counting rates of these unwanted ^{10}B ions are greater than 1 MHz. Two solutions to this problem have been adopted, depending upon whether the accelerator is large ($\geq$5 MV) or small ($\sim$2 MV).

At the final energies of 20 MeV or more achieved with the larger accelerators, the difference in stopping range of ^{10}B and ^{10}Be ions can be exploited. Boron-10 ions may be stopped in a gas cell or a foil before the detector, allowing the lower-Z ^{10}Be ions, which retain $\sim$40% of their initial energy, to be detected in an ionization chamber immediately behind the stopping region. Discrimination between ^{10}Be ions and other species such as ^9Be and ^7Be may be improved by taking two or more energy-loss signals from this detector.

Beryllium-7 ions from the $^1H(^{10}B, {}^7Be)^4He$ reaction are a potential source of background when ^{10}B fluxes are high. It is necessary, therefore, to avoid any hydrogenous component in the ^{10}B absorber. Argon is used in gas-absorber cells, and Havar (a Co/Cr/Fe/Ni/W alloy) for stopper foils or windows. An advantage of using a gas cell as the ^{10}B absorber is that it may be configured as an ion chamber. A ^{10}B flux of 10^6 s^{-1} produces an ion current of $\sim$100 nA, which not only provides an indication of the boron flux, but may also be used to tune the AMS system for optimal ^{10}Be transmission.

At the lower energies of $\sim$5 MeV available from accelerators operating at $\sim$2 MV, straggling in the range of the ^{10}B ions is too large to permit the use of a passive absorber. Instead, a 200 μg/cm^2 carbon foil is interposed in the path of the ions before the final magnetic analysis [29]. Boron-10 ions lose 300 keV more energy in this foil than do the ^{10}Be ions. Hence all but 0.2% of the ^{10}B ions are rejected in the magnet, whereas 20% of the ^{10}Be ions reach the detector. An ionization counter can then cope with the much reduced rate of ^{10}B ions, which is typically in the range of a few kHz. In this case, the full energy of the ions is deposited in the detector, allowing ready discrimination between ^{10}Be and ^{10}B ions.

The ^{10}Be/^{9}Be ratio can be determined either by injecting ^{10}BeO$^-$ and ^{9}BeO$^-$ sequentially, or by a novel simultaneous-injection method [30]. The latter exploits the fact that ^{10}Be^{16}O$^-$ and ^{9}Be^{17}O$^-$ are injected into the accelerator together and that, after acceleration, ^{17}O^{5+} ions differ by only 1% in magnetic rigidity from ^{10}Be^{3+} ions. Hence, the ^{17}O^{5+} ion current, which is a surrogate for the ^{9}Be current, can be collected continuously in an off-axis Faraday cup after the postacceleration analyzing magnet.

23.3.3 Chlorine-36 ($T_{\frac{1}{2}} = 301$ ka)

The ^{36}S isobar is the principal challenge confronting AMS measurement of ^{36}Cl. Although ^{36}S constitutes only 0.02% of natural sulfur, a mere 1 ppm of sulfur results in a ^{36}S counting rate in the detector of 1000 s^{-1}. In contrast, a typical environmental sample will have a ^{36}Cl/Cl ratio of 10^{-13} and a ^{36}Cl counting rate of only $\sim$0.5 s^{-1}. Since a sensitivity of 10^{-15} in the ratio is desirable, the detector must provide a discrimination factor of at least 10^6 between ^{36}Cl and ^{36}S ions.

Such discrimination requires the higher energies available from the larger accelerators. Effective separation is best achieved if ^{36}S penetrates significantly further into the detector than ^{36}Cl. At energies above the Bragg peak at about 24 MeV, there is a $\sim$13% difference in energy loss between ^{36}Cl and ^{36}S. If accumulated over a sufficient distance in the detector gas, this leads to a substantial spatial separation of the Bragg peaks, as illustrated in Fig. 23.4. In a detector such as that shown in Fig. 23.3, this spatial separation results in large differences in the energy-loss signals near the end of the range. The other energy-loss signals preceding the Bragg peak also provide useful discrimination. At energies above 100 MeV, rejection ratios of better than 10^6:1 are achieved at counting rates up to 10^4 s^{-1}. Although discrimination against ^{36}S is optimal for accelerators operating in excess of 10 MV, ^{36}Cl is nevertheless measured routinely at several laboratories using accelerators operating as low as 6 MV. Facilities at Purdue and Livermore carry out measurements with $\sim$60 MeV ions from FN accelerators [31,32], and measurements are conducted with 48 MeV ^{36}Cl^{7+} ions from an EN accelerator at Zürich [33]. There is also a push to perform ^{36}Cl measurements on the new generation of 5 MV
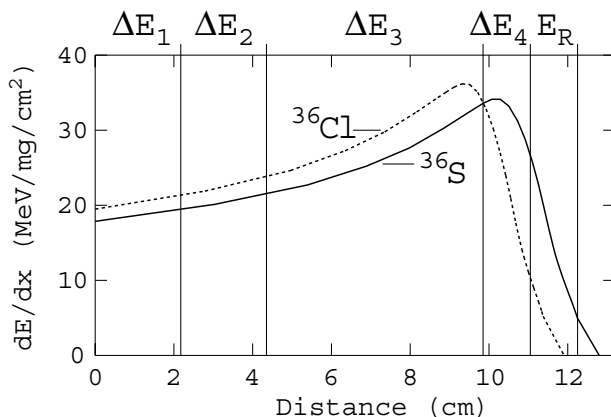
Fig. 23.4. Energy loss as a function of distance into a gas-ionization counter for 154 MeV ^{36}Cl and ^{36}S ions. The positions of the anode electrodes of the detector shown in Fig. 23.3 are indicated. Large differences between the two isotopes in the areas under the curves for individual electrodes are evident, particularly for ΔE_4 and E_R

systems, and acceptance tests for the new 5 MV system at East Kilbride in Scotland included a successful demonstration of a ^{36}Cl capability.

Clearly, it is advantageous to reduce the sulfur content of the sample as far as practicable, and this is crucial for systems operating at 5–8 MV. The silver chloride samples themselves are purified by precipitating barium sulfate from alkaline solution [34]. In addition, it is crucial to ensure that any parts of the sample holder that can be sputtered by the cesium beam are also very low in sulfur. This is achieved by masking any exposed surfaces with either silver bromide or the sample itself. Commercial silver bromide is fortuitously low in sulfur.

23.3.4 Aluminum-26 ($T_{\frac{1}{2}} = 720$ ka)

Magnesium does not form a stable negative ion. Hence, smaller as well as larger accelerators are suitable for ^{26}Al measurements. The principal limitation arises from the reluctance of aluminum to form negative ions owing to its low electron affinity (0.44 eV). Beam currents of Al$^-$ ions from Al$_2$O$_3$ samples as high as 2 μA have been reported, but 0.2–0.5 μA seems to be more typical. Consequently, and especially for geological samples which have ^{26}Al/Al ratios of less than 10^{-13}, running times per sample tend to be long, and measurement precision low. Generally, the insulating Al$_2$O$_3$ is mixed with an approximately equal weight of silver powder to ensure good electrical and thermal conduction.

An odd charge state is always employed. An even charge state, ^{26}Al^{6+} for example, would be plagued by intense counting rates of ^{13}C^{3+} from the

injection and subsequent breakup of the $^{13}C_2{}^-$ molecular ion. These ions have the same E/q and mE/q^2 as $^{26}Al^{6+}$ and therefore pass all magnetic and electric analyzers.

The AlO^- ion is produced more than an order of magnitude more prolifically than the Al^- ion. Unfortunately, MgO^- ions are also formed in the ion source, and count rates of ^{26}Mg ions at the detector are prohibitively high if the AlO^- ion is selected for injection. A possible solution would be to use a gas-filled magnet to greatly reduce the ^{26}Mg counting rate, but apart from a few measurements at Munich, this has not been seriously pursued to date, despite its obvious attractions.

23.3.5 Iodine-129 ($T_{\frac{1}{2}} = 15\,\mathrm{Ma}$)

Xenon-129 does not form a stable negative ion, and hence AMS of ^{129}I is not troubled by the stable isobar. Consequently, ^{129}I can be measured as effectively with a small accelerator as with a large one [35]. Several μA of iodine beam can be obtained from AgI samples, and sensitivities of 10^{-15} in the $^{129}I/^{127}I$ ratio are readily achievable.

Background from ^{127}I ions, which are difficult to resolve from ^{129}I in the detector, is the principal challenge to be surmounted. A very small fraction of the $^{127}I^-$ ions can acquire sufficient additional energy from the sputtering Cs^+ beam to be injected along with the ^{129}I ions. Subsequent charge-changing processes during acceleration and analysis can result in a very small, but significant, proportion of these arriving at the detector. An electrostatic analyzer (ESA) between ion source and mass-analyzing magnet eliminates this "sputter tail", and is essential on small accelerators. In the absence of such a preinjection energy analysis, the ^{127}I contribution can be minimized by sputtering with low-energy, typically $2\,\mathrm{keV}$, Cs^+ ions. Systems which employ preacceleration to $\sim100\,\mathrm{keV}$ before the magnetic mass analysis enjoy an additional advantage. At this energy, an ^{127}I ion must acquire $0.8\,\mathrm{keV}$ from the Cs^+ beam in order to be injected, whereas at the $\sim20\,\mathrm{keV}$ characteristic of the smaller accelerators, only an additional $0.16\,\mathrm{keV}$ is required. Since the probability of an energy transfer δE decreases as $\sim1/(\delta E)^2$, the number of injected $^{127}I^-$ ions is reduced by a factor of ~25 at the higher preacceleration energy.

For those systems employing a preinjection ESA, the only ions arriving at the detector with the correct charge state are ^{129}I. Lower-mass ions of the same m/q have significantly different energies and hence a detector with only modest energy resolution is sufficient.

Larger systems without a preinjection ESA generally operate at higher injection energy, and the postacceleration ESA or velocity filter is then usually sufficient to eliminate any remaining ^{127}I ions. Where this is not the case, a time-of-flight system may be employed to separate ^{129}I from those ^{127}I ions which elude the high-energy electrostatic analysis.

23.3.6 Calcium-41 ($T_{\frac{1}{2}} = 103\,\mathrm{ka}$)

A molecular negative ion is required for AMS of ^{41}Ca, owing to the very low binding energy of the atomic Ca^- ion. $\mathrm{CaH_3}^-$ has generally been the ion of choice, because the $\mathrm{KH_3}^-$ ion is not stable and hence the ^{41}K isobar is eliminated. Beam currents of several μA can be obtained from solid calcium hydride [36]. Production of calcium hydride is, however, a labor-intensive process, requiring in vacuo distillation of CaO to calcium metal.

Alternatively, the $\mathrm{CaF_3}^-$ ion may be used [37], since the $\mathrm{KF_3}^-$ ion is also unstable. The starting material is $\mathrm{CaF_2}$ which is very much simpler to produce than $\mathrm{CaH_2}$. Simplicity of sample preparation is, however, offset by the disadvantages of lower beam currents, a more extensive suite of molecular fragments, and lower final energy, and most ^{41}Ca measurements to date have employed the trihydride ion.

23.3.7 Heavy Elements ($A > 180$)

Measurement of plutonium isotopes at very low concentrations in environmental samples has provided the principal impetus to the development of AMS techniques for very heavy elements. Other isotopes such as ^{236}U, ^{237}Np, ^{226,228}Ra and ^{182}Hf have also been explored.

In the case of plutonium, there are no stable isotopes and hence no macroscopic beam to which to measure a ratio. Instead, a "spike" of a few pg of ^{242}Pu is added to the sample prior to chemical processing, and the ratios of ^{239}Pu and ^{240}Pu to ^{242}Pu are determined by ion-counting all three isotopes.

Molecular PuO^- ions are selected for injection into the accelerator. In order to minimize scattering losses, the gas stripper is operated at a thickness of $\sim 0.2\,\mu\mathrm{g/cm}^2$. The operating voltage of the accelerator is generally limited by the bending power of the postacceleration analysis system. At the ANU for example, $24\,\mathrm{MeV}$ Pu^{5+} ions are at the limit of the $ME/q^2 = 210\,\mathrm{MeV}$ amu analyzing magnet [38]. At Livermore, a $30°$ analyzing magnet permits a higher energy of $39\,\mathrm{MeV}$ [39]. Ionization chambers with an energy resolution of $\sim 3\%$ for these plutonium ions provide excellent discrimination against lower-mass ions of the same M/q arriving at the detector. Sensitivities of fewer than 10^6 atoms have been achieved for ^{239,240,242,244}Pu and ^{237}Np. For ^{239}Pu, this is two orders of magnitude better than α-particle counting.

With minor variations, the method is applicable to ^{237}Np and ^{226,228}Ra. In the former case, ^{242}Pu is again used for normalization, although ^{236}Np would be preferable if it could be obtained. In the radium case, the yield of RaO^- ions is poor, and the $\mathrm{RaC_2}$ negative ion is used instead.

Recently, it has been demonstrated that plutonium can be measured almost equally well with a small accelerator operating at only $300\,\mathrm{kV}$. The stripping yield of 3^+ ions is surprisingly high, and a gas ionization chamber with a $50\,\mathrm{nm}$ silicon nitride window provides good discrimination between $1.2\,\mathrm{MeV}$ Pu^{3+} ions and any 2^+ ions with the same mass-to-charge ratio [17].

The presence of ^{236}U is a characteristic signature of uranium that has been through a nuclear reactor, and hence this isotope is of interest in environmental and nuclear-safeguards monitoring. The much more abundant ^{238}U and ^{235}U constitute more potent sources of background than for the isotopes above, and it is necessary to supplement the total-energy measurement with a time-of-flight measurement in order to eliminate them. Sensitivities in the ^{236}U/^{238}U ratio of $\sim 10^{-12}$ have been achieved, which are sufficient for determination of ^{236}U concentrations in natural uranium ores [40].

None of the above isotopes has a stable isobar. In contrast, AMS measurement of ^{182}Hf must contend with interference from the ^{182}W isobar. At the energies available from tandem accelerators, it is not possible to separate the two, and one must rely on a background subtraction based on measured counting rates of other tungsten isotopes. Clearly, the lower the ^{182}W contribution the better, and it has been shown that use of the HfF_5^- ion suppresses the tungsten by nearly four orders of magnitude [41].

23.3.8 Other Isotopes

Techniques have been developed for the measurement of several other isotopes, but none of these has yet found wide application. For completeness, each is considered briefly below.

^{3}H ($T_{\frac{1}{2}} = 12$ a)

Decay counting is routinely used for determining tritium in water, and has high sensitivity. Nevertheless, AMS offers the advantage of smaller sample size and simpler sample preparation. At Rossendorf, a 3 MV Tandetron is used for depth profiling of tritium in carbon tiles from fusion reactor walls. Recently, this has been complemented by a small, SF_6-insulated 100 kV accelerator [42]. In addition, a tritium capability is under development on the dedicated biomedical AMS system at the Lawrence Livermore laboratory.

^{32}Si ($T_{\frac{1}{2}} = \sim 140$ a)

Silicon-32 is produced in the atmosphere by spallation of argon. Fallout is about 2 atoms/m^2/s, i.e. about 10% of ^{36}Cl. Despite the comparatively short half-life of ^{32}Si, AMS offers the advantages over conventional decay counting of smaller sample size and simpler sample preparation. It has potential for dating ice in the 50–1000 year range in temperate-zone glaciers [43], and in biomedicine [24].

A gas-filled magnet is required to separate ^{32}Si from ^{32}S ions. Fluxes of the latter are typically $>10^7$ s^{-1}. A discrimination factor of 10^{12} can be achieved with a combination of a gas-filled magnet and a suitable detector [24].

^{53}Mn ($T_{\frac{1}{2}} = 3.8$ Ma), ^{59}Ni ($T_{\frac{1}{2}} = 60$ ka), ^{60}Fe ($T_{\frac{1}{2}} = 1.5$ Ma) and ^{63}Ni ($T_{\frac{1}{2}} = 100$ a)

A gas-filled magnet has been used successfully [44] to separate these four isotopes from their stable isobars. Sensitivities of $\sim 2 \times 10^{-14}$ in the ^{53}Mn/Mn, ^{59}Ni/Ni and ^{63}Ni/Ni ratios have been achieved. For the more favorable case of ^{60}Fe, where the ^{60}Ni stable isobar differs by two in Z, sensitivity is significantly better at $\sim 2 \times 10^{-16}$.

Finally, where ^{59}Ni/Ni or ^{63}Ni/Ni ratios are $\sim 10^{-10}$ or higher as in nuclear waste, the technique of projectile X-ray emission may be employed (Sect. 23.2.2) [27, 45].

Studies of meteorites have been the principal applications of both ^{53}Mn and ^{59}Ni. Measurements of ^{60}Fe in ferromanganese crusts have provided evidence for a nearby supernova within the last 5 Ma [46]. Nickel-63, created by the ^{63}Cu(n, p)^{63}Ni reaction, is being used to check the fast-neutron dosimetry of the Hiroshima atomic bomb [47].

^{90}Sr ($T_{\frac{1}{2}} = 28.5$ a)

Strontium-90 can be measured with high sensitivity using conventional decay counting, but AMS offers the advantage of a faster response in the event of a nuclear accident. Higher energies are required in order to be able to discriminate between ^{90}Sr and its ^{90}Zr isobar. Paul et al. [48], using a ^{90}Sr energy of 131 MeV, have reported the best sensitivity to date, corresponding to ^{90}Sr/Sr $\sim 3 \times 10^{-13}$.

23.4 Applications

AMS has found application in many areas of science. In the following, a brief overview of its contribution to the most significant areas is presented.

23.4.1 Archaeology

AMS has largely supplanted liquid scintillation counting for radiocarbon dating. It offers higher throughput and smaller sample size with little or no compromise in precision. Together, these enhance the reliability of the dating by permitting more dates per site and by allowing dating of individual seeds or pieces of charcoal, for example, that are truly representative of the archaeological context. In addition, a more rigorous chemical precleaning of the sample is possible when only a milligram of carbon is sufficient.

Until recently, the expectation that the superior efficiency of the AMS technique would allow ^{14}C dating to be pushed back beyond the $\sim 50\,000$ year limit of conventional decay counting was frustrated by backgrounds due

to younger carbon that was added to a sample in the course of its history and during preparation. As the mechanisms of these processes have become better understood, however, this expectation is finally being realized [49, 50].

A few illustrative examples of the application of AMS radiocarbon dating to archaeological finds are given below.

Cave and rock art is one area where the small-sample capability of AMS allows the ^{14}C dating of the paintings themselves via milligram amounts of charcoal, or other organic matter incorporated in the pigments, without significant damage to the art. Recent spectacular cave-art finds in France at Grotte Cosquer near Marseilles and Grotte Chauvet in the Ardeche have been dated to 19 to 27 ka and 31 ka, respectively [51, 52], which are the earliest dates ever obtained for prehistoric paintings. Similar techniques are being applied to rock art in the Americas and Australia in order to shed new light on the antiquity and development of human occupation of these continents.

Another high-profile find was Ötzi, the Ice Man, whose well-preserved body was found in 1991 in the Ötztal Alps, South Tyrol, Italy. This remarkable find included clothes and shoes, a bow, a quiver of arrows, and a hand axe. AMS measurements on several artifacts, as well as on the body itself via bone and tissue specimens, place the date of his death at 4546 ± 17 radiocarbon years before present [53, 54]. This radiocarbon age translates into a calendar age between 3100 and 3350 BC.

The famous Shroud of Turin was also dated by AMS. Three laboratories each received about $2\,cm^2$ of linen from the Shroud, and their concordant results [55] pointed to a medieval date (1290–1360 AD at 90% confidence) for the Shroud. This date is close to the year 1353 when the Shroud entered the historical record.

The raw datum from a radiocarbon measurement is the ^{14}C/^{12}C ratio. Since this ratio in atmospheric CO_2 has not been constant in time but has fluctuated in response to a number of factors, including solar activity and the geomagnetic field, the relationship between the measured ratio and the calendar age of the sample is not a simple one. Natural archives which can be precisely dated by other means are required in order to calibrate the radiocarbon timescale in terms of calendar time.

Tree rings, for which a continuous annual record is now available back to 12 400 years before present, have allowed the construction of a high-precision calibration curve from the late-glacial period to the present [56]. A section of the curve is shown in Fig. 23.5. Beyond the tree ring record, other archives are required. These include corals, which can be U/Th dated, annually laminated lake and marine sequences, and marine sediments with chronologies tied to "well-dated" Greenland ice cores via fluctuations in the ^{18}O to ^{16}O isotope ratio. A reasonable consensus exists back to ∼26 ka, but the different archives diverge significantly between 26 and 40 ka.
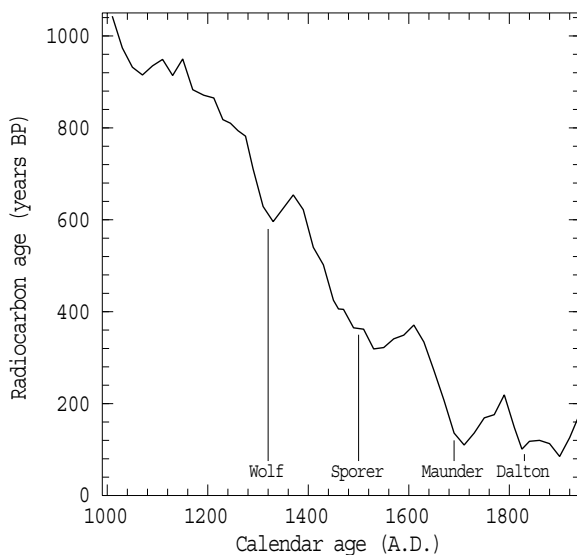
Fig. 23.5. The portion of the ^{14}C calibration curve from 1000 to 1920 AD. Minima in this curve, which correspond to periods of elevated ^{14}C production, line up with the well-known minima in sunspot activity. (After [56])

23.4.2 Exposure-Age Dating

Secondary cosmic rays, principally fast neutrons and muons, produce the long-lived isotopes ^{10}Be, ^{26}Al and ^{36}Cl in situ by interactions with suitable target nuclei in surface rocks. Provided that the production rates are known, the buildup of one or more of these isotopes may be used to determine the time of first exposure of the rock at the earth's surface. Direct dating of the advance and retreat of glaciers using either transported boulders or polished bedrock surfaces is providing essential paleoclimatic data for testing models of the earth's climate. Other geological processes or features such as meteorite impacts, fault movements, lava flows and landslides, and wave-cut platforms can also be dated. In addition, erosion rates can be determined for surfaces that have been exposed for long enough to have attained saturation to provide information on landscape evolution on 100 ka to 10 Ma year timescales. For a recent review of this rapidly expanding field, see Gosse and Phillips [11].

23.4.3 Ice Cores

Polar ice preserves a continuous record of the ^{10}Be and ^{36}Cl which are produced by cosmic-ray interactions in the atmosphere. Detailed studies of these isotopes are providing valuable information about past variations in solar activity, the strengths of the terrestrial and solar magnetic fields, and their links to climate [57].

Ice cores are also unique archives of anthropogenic ^{36}Cl. Nuclear-weapons testing in the late 1950s injected large quantities of ^{36}Cl into the stratosphere, where it was well mixed before falling out. Ice cores from high-accumulation sites such as Dye three in Greenland preserve an annual record of this fallout, which at its peak was three orders of magnitude above the normal cosmogenic rate [58] (see Fig. 23.6).
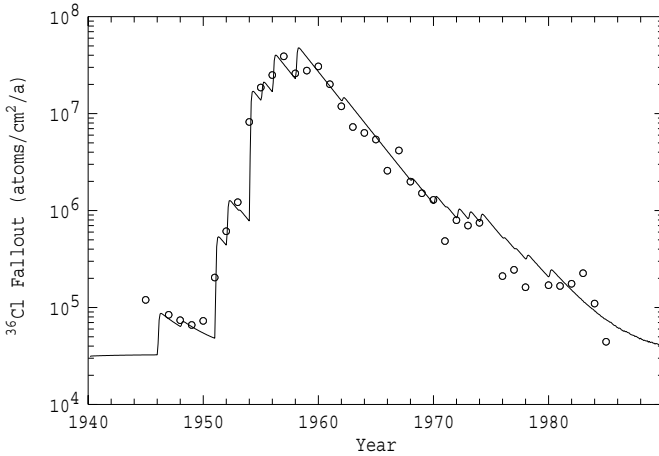

Fig. 23.6. The ^{36}Cl bomb pulse in an ice core from Dye 3, Greenland. The solid line is the result of a box-model calculation which incorporates the various test explosions (after [58])

23.4.4 Deep-Sea Cores

Cores from ocean sediments are providing a wealth of information about past climates, particularly over the 120 ka span of the most recent glacial cycle. Establishing an absolute chronology for these stages has, however, proved to be difficult. Fortunately, the most recent part of the record, which embraces the abrupt end about 15 ka ago of the last major glaciation, and the brief return of cold conditions about 11 ka ago during the Younger Dryas period, falls within the range of radiocarbon dating. AMS, because it permits the dating of individual species of foraminifera hand-picked from cores, has been instrumental in the construction of accurate chronologies spanning these changes [59].

23.4.5 Oceanography

A very large number of ^{14}C measurements have been performed by the National Ocean Sciences AMS facility at the Woods Hole Oceanographic Institute as part of the World Ocean Circulation Experiment (WOCE) [60].

Questions being addressed are the turnover and mean residence times of deep ocean water, mixing between basins, and the transfer of heat from low to high latitudes. Bomb-produced ^{14}C has provided valuable information about surface ocean circulation and atmosphere–ocean exchange processes, and here the amplitude of the signal is more than 20%. The bomb pulse has not yet penetrated into the deep basins of the world's oceans, and lateral gradients there are due to mixing of waters which were last exposed to atmospheric exchange at different times. Gradients are typically only 2 to 3% across an entire basin, and 0.3–0.4% precision is required. An AMS measurement needs only 0.5 l of water, which greatly simplifies sample collection and storage compared with the 200 l that were formerly required for decay counting.

Knowledge of present-day circulation in the Arctic Ocean is crucial to understanding heat transfer from low to high latitudes. Serendipitously, nuclear-fuel reprocessing plants at Sellafield in Cumbria (UK) and La Hague on the Cherbourg Peninsula (France) have, since 1954 and 1970 respectively, been potent point sources of ^{129}I and ^{99}Tc. Currents running through the English Channel and up the west coast of the UK have carried these isotopes into the Arctic Ocean. Surveys of ^{129}I levels, both in surface waters over an extended area and as a function of depth, are providing valuable insights into circulation patterns and vertical mixing in this important area [61], and work is under way to complement these with ^{99}Tc.

23.4.6 Biomedicine

Liquid scintillation counting of ^{14}C is very widely employed in biomedical research and in drug testing. AMS offers the major advantage of requiring very much smaller doses, thereby reducing both the expense of labeled compounds and the problems of disposal, and allowing studies in humans. The high throughput of AMS is also highly advantageous, since meaningful conclusions can only be drawn from studies which incorporate large numbers of subjects and controls. Pioneering work in this area has been directed towards measuring, at environmentally realistic doses, the rates at which known mutagens bind to DNA [62]. AMS facilities dedicated to biomedical applications have been constructed at the University of York (UK), Lawrence Livermore Laboratory and MIT. Recently, considerable progress has been made in coupling gas and liquid chromatographs directly to an AMS system to allow on-line compound-specific ^{14}C analyses [63].

23.4.7 Hydrology

Chlorine-36 is the principal AMS isotope used in hydrology. A useful review has been given by Fontes and Andrews [64]. It has found application in determining the age of groundwater, in measuring recharge rates, in studying past climates, and in investigating the hydrology of nuclear-waste analogues and potential waste disposal sites.

Extensive use of ^{129}I, often accompanied by ^{36}Cl, has also been made to investigate the origins and residence times of hydrothermal fluids and oil-field brines [65].

23.4.8 Extraterrestrial Material

AMS studies of long-lived isotopes such as ^{10}Be, ^{14}C, ^{26}Al, ^{36}Cl, ^{41}Ca and ^{59}Ni in meteorites have been directed towards establishing the nonterrestrial origin of a putative meteorite, determining the irradiation history of the parent body in space, and establishing the time at which a given meteorite fell to earth. A useful review has been given by [66].

23.5 Conclusions and Prospects

In the 26 years since the first demonstration that ^{14}C could be detected at natural levels using an electrostatic tandem accelerator, the field of accelerator mass spectrometry has expanded into many areas of science. Despite its maturity, growth continues at a rapid pace. There is a strong push towards smaller, cheaper systems; techniques for new isotopes are continually being developed; and new facilities are proliferating. In parallel, there is increasing sophistication in the area of applications, often driving improvements in technique.

References

1. D E Nelson, R G Korteling, W R Stott: Science **198**, 507 (1977)
2. C L Bennett, R P Beukens, M R Clover, H E Gove, R B Liebert, A E Litherland, K H Purser, W E Sondheim: Science **198**, 508 (1977)
3. K H Purser, R B Liebert, C J Russo: Radiocarbon **27**, 794 (1980)
4. D Elmore, B R Fulton, M R Clover, J R Marsden, H E Gove, K H Purser, L R Kilius, R Beukens, A E Litherland: Nature **277**, 22 (1979)
5. D Elmore, H E Gove, R Ferraro, L R Kilius, H W Lee, K H Chang, R P Beukens, A E Litherland, C J Russo, K H Purser, M T Murrell, R C Finkel: Nature **286**, 138 (1980)
6. J Klein, R Middleton, H Tang: Nucl. Instr. Meth. Phys. Res. **193**, 601 (1982)
7. R Middleton, J Klein, G M Raisbeck, F Yiou: Nucl. Instr. Meth. Phys. Res. **218**, 430 (1983)
8. R C Finkel, M Suter: Adv. Anal. Chem. **1**, 1 (1993)
9. C Tuniz, J R Bird, D Fink, G F Herzog: *Accelerator Mass Spectrometry: Ultrasensitive Analysis for Global Science* (Boca Raton, FL: CRC Press) (1998)
10. L K Fifield: Rep. Prog. Phys. **62**, 1223 (1999)
11. J Gosse, F M Phillips: Quaternary Sci. Rev. **20**, 1475 (2001)
12. C Bronk-Ramsey, R E M Hedges: Nucl. Instr. Meth. Phys. Res. B **123**, 539 (1997)

13. J R Southon, D E Nelson, J S Vogel: Nucl. Instr. Meth. Phys. Res. B **52**, 370 (1990)
14. K H Purser, T H Smick, R K Purser: Nucl. Instr. Meth. Phys. Res. B **52**, 263 (1990)
15. M Suter, S W A Jacob, H A Synal: Nucl. Instr. Meth. Phys. Res. B **172**, 144 (2000)
16. H-A Synal, M Dobeli, S Jacob, M Stocker, M Suter: Nucl. Instr. Meth. Phys. Res. B **223–224**, 339–345 (2004)
17. L K Fifield, H A Synal, M Suter: Nucl. Instr. Meth. Phys. Res. B **223–224**, 802–806 (2004)
18. M Suter, G Bonani, C Stoller, W Wölfli: Nucl. Instr. Meth. B **5**, 251 (1984)
19. G Bonani, P Eberhardt, H J Hofmann, T H Niklaus, M Suter, H A Synal, W Wölfli: Nucl. Instr. Meth. Phys. Res. B **52**, 338 (1990)
20. E Boaretto, D Berkovits, G Hollos, M Paul: Nucl. Instr. Meth. Phys. Res. B **50**, 280 (1990)
21. M Paul: Nucl. Instr. Meth. Phys. Res. B **52**, 315 (1990)
22. U Zoppi, P W Kubik, M Suter, H A Synal, H R von Gunten, D Zimmerman: Nucl. Instr. Meth. Phys. Res. B **92**, 142 (1994)
23. K Knie, T Faestermann, G Korschinek: Nucl. Instr. Meth. Phys. Res. B **123**, 128 (1997)
24. J Popplewell, S J King, J P Day, P Ackrill, L K Fifield, R G Cresswell, M L di Tada, K Liu: J. Inorg. Biochem. **69**, 177 (1998)
25. H Artigalas, J L Debrun, L Kilius, X L Zhao, A E Litherland, J L Pinault, C Fouillac, C J Maggiore: Nucl. Instr. Meth. Phys. Res. B **92** 227 (1994)
26. M J M Wagner, H A Synal, M Suter, J L Debrun: Nucl. Instr. Meth. Phys. Res. B **99**, 519 (1995)
27. J E McAninch, L J Hainsworth, A A Marchetti, M R Leivers, P R Jones, A E Dunlop, R Mauthe, J S Vogel, I D Proctor, T Straume: Nucl. Instr. Meth. Phys. Res. B **123**, 137 (1997)
28. D Fink, B McKelvey, D Hannan, D Newsome: Nucl. Instr. Meth. Phys. Res. B **172**, 838 (2000)
29. G M Raisbeck, F Yiou, D Bourles, J Lestringuez, D Deboffle: Nucl. Instr. Meth. Phys. Res. B **5**, 175 (1984)
30. R Middleton, J Klein: Phil. Trans. Roy. Soc. Lond. A **323**, 121 (1987)
31. D L Knies, D Elmore: Nucl. Instr. Meth. Phys. Res. B **92**, 134 (1994)
32. M L Roberts et al.: Nucl. Instr. Meth. Phys. Res. B **123**, 57 (1997)
33. H A Synal, J Beer, G Bonani, C Lukasczyk, M Suter: Nucl. Instr. Meth. Phys. Res. B **92**, 79 (1994)
34. N J Conard, D Elmore, P W Kubik, H E Gove, L E Tubbs, B A Chrunyk, M Wahlen: Radiocarbon **28**, 556 (1986)
35. L R Kilius, N Baba, M A Garwan, A E Litherland, M-J Nadeau, J C Rucklidge, G C Wilson, X L Zhao: Nucl. Instr. Meth. Phys. Res. B **52**, 357 (1990)
36. D Fink, R Middleton, J Klein: Nucl. Instr. Meth. Phys. Res. B **47**, 79 (1990)
37. S P H T Freeman, J S Vogel: Mass Spectrom. Ion Proc. **143**, 247 (1995)
38. L K Fifield, A P Clacher, K Morris, S J King, R G Cresswell, J P Day, F R Livens: Nucl. Instr. Meth. Phys. Res. B **123**, 400 (1997)
39. J E McAninch et al.: Nucl. Instr. Meth. Phys. Res. B **172**, 711 (2000)
40. P Steier, R Golser, W Kutschera, V Liechtenstein, A Priller, A Valenta, C Vockenhuber: Nucl. Instr. Meth. Phys. Res. B **188**, 283 (2002)

41. C Vockenhuber, M Bichler, R Golser, W Kutschera, A Priller, P. Steier, S. Winkler: Nucl. Instr. Meth. Phys. Res. B **223–224**, 823–828 (2004)
42. M Friedrich, W Pilz, G Sun, R Behrisch, C Garcia-Rosales, N Bekris, R D Penzhorn: Nucl. Instr. Meth. Phys. Res. B **172**, 655 (2000)
43. U Morgenstern, L K Fifield, A Zondervan: Nucl. Instr. Meth. Phys. Res. B **172**, 605 (2000)
44. K Knie, T Faestermann, G Korschinek, G Rugel, W Ruhm, C Wallner: Nucl. Instr. Meth. Phys. Res. B **172**, 717 (2000)
45. P Persson, M Kiisk, B Erlandsson, M Faarinen, R Hellborg, G Skog, K Stenström: Nucl. Instr. Meth. Phys. Res. B **172**, 188 (2000)
46. K Knie, G Korschinek, T Faestermann, C Wallner, J Scholten, W Hillebrandt: Phys. Rev. Lett. **83**, 18 (1999)
47. T Straume et al. : Nature **424**, 539 (2003)
48. M Paul, D Berkovits, L D Cecil, H Feldstein, A Hershkowitz, Y Kashiv, S Vogt: Nucl. Instr. Meth. Phys. Res. B **123**, 394 (1997)
49. M I Bird, L K Ayliffe, L K Fifield, C S M Turney, R G Cresswell, T T Barrows, B David: Radiocarbon **41**, 127 (1999)
50. M J Nadeau, P M Grootes, A Voelker, F Bruhn, A Duhr, A Oriwall: Radiocarbon **43**, 169 (2001)
51. J Clottes, J Courtin, H Valladas, H Cachier, N Mercier, M Arnold: Bull. Soc. Préhistorique Française **89**, 270 (1992)
52. J Clottes, J M Chauvet, E Brunel-Deschamps, C Hillaire, J P Daugas, M Arnold, H Cachier, J Evin, P Fortin, C Oberlin, N Tisnerat, H Valladas: C.R. Acad. Sci. Paris **320**, 1133 (1995)
53. R E M Hedges, R A Housley, C R Bronk, G J van Klinken: Archaeometry **34**, 337 (1992)
54. G Bonani, S D Ivy, I Hajdas, T R Niklaus, M Suter: Radiocarbon **36**, 247 (1994)
55. P E Damon, D J Donahue, B H Gore, A L Hatheway, A J T Jull, T W Linick, P J Sercel, L J Toolin, C R Bronk, E T Hall, R E M Hedges, R Housley, I A Law, C Perry, G Bonani, S Trumbore, W Woelfli, F C Ambers, S G E Bowman, M N Leese, M S Tite: Nature **337**, 611 (1989)
56. M Stuiver, P J Reimer, J W Beck, E Bard, G S Burr, K A Hughen, B Kromer, F G McCormack, J van der Plicht, M Spurk: Radiocarbon **40**, 1041 (1998)
57. J Beer: Space Sci. Rev. **11**, 53 (2000)
58. H A Synal, J Beer, G Bonani, M Suter, W Wölfli: Nucl. Instr. Meth. Phys. Res. B **52**, 483 (1990)
59. K A Hughen, J R Southon, S J Lehman, J T Overpeck: Science **290**, 1951 (2000)
60. K F Von Reden, A P McNichol, J C Peden, K L Elder, A R Gagnon, R J Schneider: Nucl. Instr. Meth. Phys. Res. B **123**, 438 (1997)
61. G M Raisbeck, F Yiou: Sci. Total Environ. **237/238**, 31 (1999)
62. J S Vogel: Nucl. Instr. Meth. Phys. Res. B **172**, 884 (2000)
63. P L Skipper, B J Hughey, R G Liberman, M H Choi, J S Wishnok, R E Klinkowstein, R E Shefer, S R Tannenbaum: Nucl. Instr. Meth. Phys. Res. B **223–224**, 740–744 (2004)
64. J C Fontes, J N Andrews: Nucl. Instr. Meth. Phys. Res. B **92**, 367 (1994)
65. J E Moran, U Fehn, J S Hanor: Geochim. Cosmochim. Acta **59**, 5055 (1995)
66. G F Herzog: Nucl. Instr. Meth. Phys. Res. B **92**, 478 (1994)